Heat Transport in Spin Chains with Weak Spin-Phonon Coupling

A. L. Chernyshev[1] and A. V. Rozhkov[2,3]
[1]Department of Physics and Astronomy, University of California, Irvine, California 92697, USA
[2]Moscow Institute of Physics and Technology, Dolgoprudny, Moscow Region 141700, Russia
[3]Institute for Theoretical and Applied Electrodynamics, Russian Academy of Sciences, Moscow 125412, Russia
(Received 9 September 2015; published 8 January 2016)

The heat transport in a system of $S = 1/2$ large-J Heisenberg spin chains, describing closely Sr_2CuO_3 and $SrCuO_2$ cuprates, is studied theoretically at $T \ll J$ by considering interactions of the bosonized spin excitations with optical phonons and defects. Treating rigorously the multiboson processes, we derive a microscopic spin-phonon scattering rate that adheres to an intuitive picture of phonons acting as thermally populated defects for the fast spin excitations. The mean-free path of the latter exhibits a distinctive T dependence reflecting a critical nature of spin chains and gives a close description of experiments. By the naturalness criterion of realistically small spin-phonon interaction, our approach stands out from previous considerations that require large coupling constants to explain the data and thus imply a spin-Peierls transition, absent in real materials.

DOI: 10.1103/PhysRevLett.116.017204

The one-dimensional (1D) spin chains are among the first strongly interacting quantum many-body systems ever studied [1,2], and they remain a fertile ground for new ideas [3] and for developments of advanced theoretical and numerical [4,5] methods. A number of physical realizations of spin-chain materials [6–10] have allowed for unprecedentedly comprehensive comparisons between theory, numerical approaches, and experimental data [11–13]. Current theoretical challenges for these systems include their dynamical, nonequilibrium, and transport properties [14–20]. The transport phenomena are particularly challenging as the couplings to phonons and impurities, perturbations that are extrinsic to the often integrable spin systems, become crucial [21–26].

In this Letter, we address the problem of heat transport in 1D spin-chain systems by considering coupling of spins to optical phonons and impurities and having in mind a systematic, experimental thermal conductivity study in the high-quality single-crystalline, large-J spin-chain cuprates Sr_2CuO_3 and $SrCuO_2$ that has been recently conducted [27–30]. Several attempts to develop a suitable formalism to describe this phenomenon have been made in the past [24–26]. However, these approaches either relied on unrealistic choices of parameters [24,26] or offered only qualitative insights [24,25].

Below, we attempt to bridge the gap between experiment and theory. We argue that the heat conductivity by spin excitations can be quantitatively described within the bosonization framework with the large-momentum scattering by optical phonons or impurities. For weak impurities, scattering grows stronger at lower temperature, a feature intimately related to a critical character of the $S = 1/2$ Heisenberg chains [26]. Taking into account multi-spin-boson processes, it follows naturally from our microscopic calculations that scattering by phonons bears a close similarity to that by weak impurities, except that the phonons are thermally populated and thus control heat transport at high T. This is also in accord with a physical picture of phonons playing the role of impurities for the fast spin excitations. Within this picture, the transport relaxation time is the same as spin-boson scattering time and the corresponding mean-free path fits excellently the available experimental data. Further systematic extensions of our theory to include multiphonon scattering that can influence thermal conductivity at higher temperature are briefly discussed.

Finally, we emphasize an important physical constraint on the strength of spin-phonon coupling of a magnetoelastic nature [31,32], which is weak in the materials of interest. While an estimate of this coupling can be made microscopically, a simple piece of phenomenological evidence for this criterion is the absence of the spin-Peierls transition in real compounds down to very low temperatures. Our theory easily satisfies the proposed constraint, setting itself apart from the previous approaches [24,26]. We thus provide a microscopic, internally consistent description of thermal transport and scattering in 1D spin chains, which satisfies naturalness criteria by having weak spin-phonon coupling and conforming to an analogy between phonon and impurity scatterings.

Spin-phonon coupling Hamiltonian.—The nearest-neighbor Hamiltonian of an $S = 1/2$ Heisenberg chain magnetoelastically coupled to phonons is

$$\mathcal{H} = \sum_{\langle ij \rangle} J(\mathbf{r}_i - \mathbf{r}_j)\mathbf{S}_i \cdot \mathbf{S}_j, \tag{1}$$

where $\langle ij \rangle$ denotes nearest-neighbor lattice sites. A standard Jordan-Wigner transformation with the subsequent bosonization [11] and the lowest-order expansion in lattice displacements brings it to the following form:

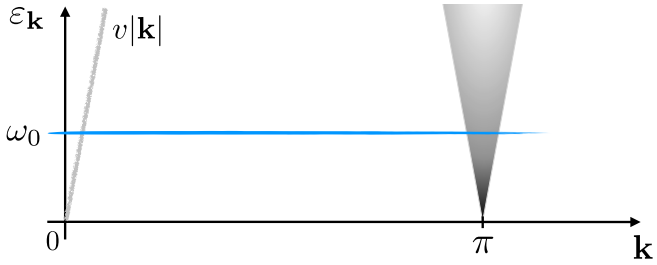

FIG. 1. Schematics of the spectra of bosonic excitations in a large-J, $S = 1/2$ Heisenberg spin chain (dispersive branch $\varepsilon_{\mathbf{k}} = v|\mathbf{k}|$ and a continuum at $\mathbf{Q} = \pi$) and of the dispersionless optical phonon branch ω_0 (the horizontal line).

$$\mathcal{H} = \sum_k \varepsilon_k b_k^\dagger b_k + \mathcal{H}_{\text{s-ph}}, \tag{2}$$

where $b_k^{(\dagger)}$ represents spin-boson operators of the excitation with $\varepsilon_k = v|k|$ (sketched in Fig. 1), velocity is $v = \pi J a/2$, k is the 1D momentum, and a is the lattice spacing. Hamiltonian $\mathcal{H}_{\text{s-ph}}$ describes a large-momentum, $q \approx Q = \pi/a$, spin-boson scattering by phonons

$$\mathcal{H}_{\text{s-ph}} = \frac{2\lambda}{\pi a^2} \int dx \mathbf{U}_x(x) \cos(\hat{\Phi}(x) + Qx), \tag{3}$$

where $\lambda = a\partial J/\partial x$, x is the direction along the chains, the lattice displacement field $\mathbf{U}(x)$ is associated with the optical and zone boundary phonons, and the spin-boson field $\hat{\Phi}(x) = \sqrt{\pi}\sum_k e^{ikx}(b_k^\dagger + b_{-k})/\sqrt{L|k|}$, in which L is the linear size of the chain and we used the Luttinger-liquid parameter $\mathcal{K} = 1/2$ for the Heisenberg case [33]. Small-momentum scattering is deliberately ignored, as the corresponding vertex carries small in-plane momentum of the phonon and leads to negligible scattering effects [26].

We note that boson-boson scattering cannot dissipate the heat current [21,22,35] and thus is neglected.

Self-energy and relaxation rate.—Assuming the spin-phonon coupling to be small, a conjecture discussed below in detail [32], one can consider only the second-order spin-boson self-energy in Fig. 2(a) given by

$$\Sigma_k(\tau) = -\frac{2\lambda^2}{\pi a^4 |k|} \int dx e^{ikx} D(\tau, x) \langle e^{-i\hat{\Phi}(0,0)} e^{i\hat{\Phi}(\tau,x)} \rangle, \tag{4}$$

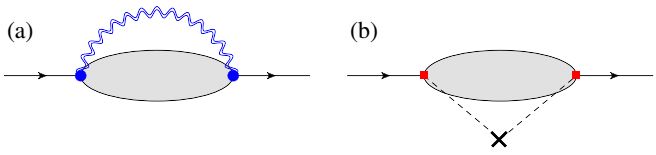

FIG. 2. Multiboson diagrams contributing to the scattering rate of spin bosons on (a) phonons and (b) weak impurities. Shaded ellipses represent a set of diagrams involving an arbitrary number of spin bosons in the intermediate state. Solid and wavy lines are the Green's functions of spin bosons and phonons, respectively.

where $D(\tau, x) = \langle \mathbf{U}_x(0,0)\mathbf{U}_x(\tau, x)\rangle$ is the phonon propagator and the second quantization of the lattice-displacement field is standard [36]. We exploit the large value of J compared to a typical Debye energy (in cuprates $J/\Theta_D \sim 10$), which allows us to neglect dispersion of the phonon branches near the π point in Fig. 1. Then, the lattice-displacement correlator is fully local in space [33] and separates into a sum over phonon branches ℓ that have nonzero projections of their polarizations, $\boldsymbol{\xi}^x_{\mathbf{q}\ell}$, on the chain axis x. Considering for simplicity only one longitudinal phonon with the energy ω_0 (see Fig. 1), and reserving the right to add more phonon branches later, we obtain $D(\tau, x) = a\delta(x)F_\tau(\omega_0)/2m\omega_0$ with

$$F_\tau(\omega_0) = n_0 e^{\omega_0 \tau} + (n_0 + 1)e^{-\omega_0 \tau}, \tag{5}$$

where $n_0 = 1/(e^{\omega_0/T} - 1)$ is the phonon distribution function, m is the mass of the unit cell, and $\hbar = k_B = 1$.

For the bosonic field correlator in the spin-phonon self-energy (4) in Fig. 2(a), we note an immediate similarity to the second-order T matrix for the weak impurity scattering in Fig. 2(b), which also generates a large-momentum transfer [26]. The correlator can be evaluated at $x \to 0$ and $T \ll J$ [26,33] and leads to

$$\langle e^{-i\hat{\Phi}(0,0)} e^{i\hat{\Phi}(\tau,0)} \rangle \approx \frac{\pi T}{J|\sin(\pi T \tau)|}. \tag{6}$$

Then, the self-energy at Matsubara frequency ω_n is

$$\Sigma_k(\omega_n) = -g_{\text{sp}}^2 \frac{2TJ}{a|k|} \int_0^\beta d\tau \frac{e^{i\omega_n \tau} - 1}{|\sin(\pi T \tau)|} F_\tau(\omega_0), \tag{7}$$

where we introduced a naturally appearing *dimensionless* spin-phonon coupling constant $g_{\text{sp}} = \lambda/(aJ\sqrt{2m\omega_0})$ [31,32]. For the spin-boson scattering rate, we need the imaginary part of the self-energy that is analytically continued to real frequencies. The transformations allowing us to perform the integration in Eq. (7) exactly are delegated to the Supplemental Material [33]. Here, we simply list the answer,

$$\text{Im}\Sigma_k(\omega) = -g_{\text{sp}}^2 \frac{2J}{a|k|}(2n_0 + 1)(1 - f_+ - f_-), \tag{8}$$

where $f_\pm = 1/(e^{\omega \pm \omega_0} + 1)$. The fermionic distributions can be seen as a result of a refermionization of bosons via a multiple-boson scattering. The result (8) can be expanded in ω/T, yielding

$$\text{Im}\Sigma_k(\omega) \approx -g_{\text{sp}}^2 \frac{2J\omega}{a|k|T} \frac{1}{\sinh(\omega_0/T)}, \tag{9}$$

which holds exceptionally well for all $\omega \lesssim T$ of interest. Generally, the single-particle scattering rate (9) should differ from the transport relaxation rate, but for the impuritylike scattering the two become the same.

Mean-free path.—Then, the on-shell approximation, $\omega = \varepsilon_k$, in Eq. (9) yields the inverse spin-boson mean-free path, $1/\ell = 1/v\tau$, due to spin-phonon scattering:

$$\left(\frac{\ell_{\rm sp}}{a}\right)^{-1} = g_{\rm sp}^2 \frac{2J}{T} \frac{1}{\sinh(\omega_0/T)}. \quad (10)$$

This result is k independent and thus can be compared directly to the transport mean-free path extracted from thermal conductivity data [27,29]. We note that the $1/T$ prefactor in Eq. (10) is strongly reminiscent of the result for the scattering on weak impurities [26,37,38]: $(\ell_{\rm imp}/a)^{-1} = n_{\rm imp}(\delta J/J)^2(J/T)$, where $n_{\rm imp}$ is the concentration of such impurities and δJ is the strength of impurity potential. Clearly, this scattering gets stronger with lowering T, down to the Kane-Fisher scale, $T_{\rm KF} \propto \delta J^2/J$, below which weak impurity becomes a strong scatterer, similar to a chain break [39]. This behavior is a consequence of a critical character of spin chains [26,40]. Since phonons should be seen as weak impurities by the fast spin excitations, it is natural that the spin-phonon scattering yields the same $1/T$ prefactor in Eq. (10).

While the other thermal factor in Eq. (10), $1/\sinh(\omega_0/T)$, does not coincide with the phonon population n_0, both have the same high- and low-T asymptotes. For $T \ll \omega_0$, the mean-free path (10) exhibits activated behavior, $\ell_{\rm sp} \sim e^{\omega_0/T}$, similar to the findings of other works [24,25].

In addition to the considered scattering mechanisms, the low-T spin thermal conductivity in real materials is limited by strong defects that act like chain breaks [27,28,30]. The corresponding mean-free path is an average length of a defect-free chain segment, $1/\ell_{\rm b} = n_{\rm b}$, where n_b is the concentration of these defects.

Comparison with experiments.—Figure 3 shows the T dependence of the mean-free path of 1D spin excitations in Sr_2CuO_3 and $SrCuO_2$ [27,29]. The data are extracted from the thermal conductivity measurements via a kinetic relation, $\ell(T) = \kappa(T)/vC_V(T)$, using theoretical values [41] for the specific heat of spin chains $C_V(T)$ [$\propto T$ at $T \ll J$]. Because of high purity, the mean-free path exceeds $10^3 a$ at low T, with the difference between the two compounds due to the residual concentrations of the defects. The two sets of data become quantitatively very close at higher T, implying that a similar scattering is dominating propagation of heat in both materials [29].

Figure 3 shows our successful fits of the data by combining spin-phonon (10) and strong-impurity scatterings, $\ell^{-1} = \ell_{\rm sp}^{-1} + \ell_{\rm b}^{-1}$, via Matthiessen's rule [27]. We note that the low-T part of the data, $T \lesssim 40$ K, has a large uncertainty due to the subtraction of the phonon part of the thermal conductivity (see [27,29]), and that it can be fit with equal success by a combination of weak and strong impurities, $\ell^{-1} \approx \ell_{\rm imp}^{-1} + \ell_{\rm b}^{-1}$. Since it is a secondary issue for our study, the simplest account of this regime by strong impurities suffices. To fit the spin-boson mean-free path above 40 K, we assume that the spin bosons are scattered by two phonon modes with $\omega_{0,1} = 300$ K and $\omega_{0,2} = 740$ K. Of the two, the first roughly corresponds to the longitudinal zone-boundary phonon and the second to the high-energy stretching mode [42,43], both likely having the strongest coupling to spin chains. In Eq. (10) we used the value of

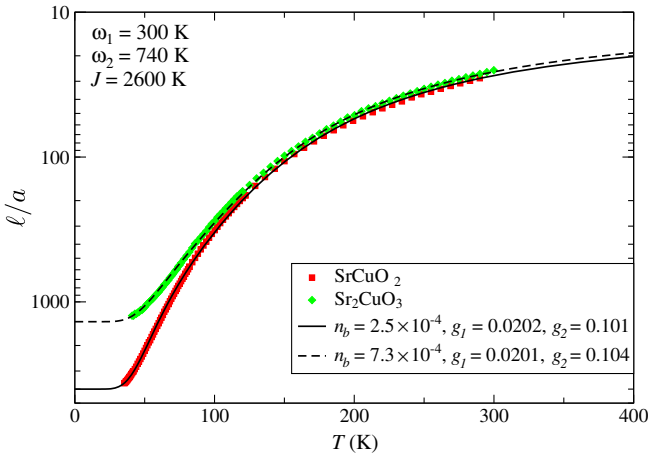

FIG. 3. Mean-free path of spin excitations in Sr_2CuO_3 and $SrCuO_2$ [27–29] (the symbols). Lines are theory fits; see the text. Concentrations of strong impurities, $n_{\rm b}$, phonon energies, $\omega_{0,i}$, and spin-phonon coupling constants, $g_{i,\rm sp}$, are as indicated in the graph.

$J = 2600$ K [44] and the spin-phonon coupling constants $g_{1,\rm sp} = 0.020(1)$ and $g_{2,\rm sp} = 0.10(1)$ have provided the fit in Fig. 3 for Sr_2CuO_3 and $SrCuO_2$. By choosing different $\omega_{0,i}$'s, one can obtain somewhat different values of the $g_{i,\rm sp}$'s needed for the fit, but they never exceed or even reach the physical bounds discussed next.

Bounds on spin-phonon coupling.—We now discuss physical bounds on the spin-phonon coupling constant $g_{\rm sp} = \lambda/(Ja\sqrt{2m\omega_0})$. As discussed in Refs. [31,32], the constant is a product of two parameters, with one characterizing the change of J by atomic displacement, $\gamma = \lambda/J = a(\partial J/\partial x)/J$, and the other representing an amplitude of zero-point atomic motion relative to a lattice constant [36], $\alpha = \hbar/\sqrt{2ma^2\omega_0}$, where $\hbar$ is made explicit and m is the reduced mass associated with the phonon mode ω_0. Parameter α is small, while γ can be large [31,43] because the superexchange is sensitive to the interatomic distance. Regarding cuprates, one can estimate $\alpha \approx 0.01$. The superexchange parameter has a larger uncertainty, with indirect studies giving a range of $\gamma = 3$–14 [43,45] and a consideration of a wider class of materials suggesting an upper limit of $\gamma \leq 20$ [31]. Thus, the microscopic upper bound on the spin-phonon coupling constant in 1D cuprates can be put at $g_{\rm sp}^{\rm max} \approx 0.2$, justifying the weak-coupling treatment of the spin-boson scattering on phonons in Eq. (4).

A less restrictive, but purely phenomenological criterion limiting the strength of the spin-phonon coupling is the absence of the spin-Peierls transition in 1D cuprates down to about 5 K ($\approx 0.002J$), where the 3D Néel ordering can be argued to preempt other transitions. Using $T_{\rm P} \approx Je^{-1/g_{\rm sp}^2}$, this can be translated to the upper limit on the spin-phonon coupling $g_{\rm sp}^{\rm max} \approx 0.35$.

We now offer a critique of the previous considerations of thermal transport in 1D spin chains. In particular, in experimental works [27,29,44], the spin-phonon mean-free

path is repeatedly fit by the form $\ell_{\rm sp}^{-1} = ATe^{-\omega^*/T}$, with $\omega^* \approx 200$ K, inspired by the phonon-mediated Umklapp scenario [24]. First, most of the data in Fig. 3 should be outside the quantitative accuracy range of this expression, which is limited to $T \lesssim \omega^*/3 \approx 70$ K, as the exponent is only a low-T limit of the phonon distribution function. More importantly, translating the values of A used in Refs. [27,29,44] to the dimensionless coupling constant via $A = g_{\rm sp}^2/Ja$ gives $g_{\rm sp} \approx 1$, which is exceedingly large for the perturbative treatment to hold and lies way outside the allowed range. This strong coupling also implies a spin-Peierls transition at $T_{\rm P} \sim J$, while no such transition is observed. Likewise, our previous study, which considered small-momentum scattering on acoustic phonon branches [26], required an anomalously strong spin-phonon interaction $g_{\rm sp} > 1$. Thus, there is a serious "naturalness" problem with previous theoretical considerations.

In the present work, the dimensionless spin-phonon coupling constants are well within the range of the microscopic expectations for the cuprates, $g_{\rm sp} = 0.02$–0.1, implying extremely low spin-Peierls transition temperatures. While the offered analysis of the physical bounds is not a proof of the validity of our theory, it is certainly a strong argument against the validity of the previous approaches, which require unphysically large spin-phonon coupling.

Multiphonon scattering.—We note that for $T \gtrsim \omega_0$ the spin-boson mean-free path in Eq. (10) saturates at $(\ell_{\rm sp}/a)^{-1} \approx g_{\rm sp}^2 2J/\omega_0$. While this is not unphysical, one can still expect that the other, T-dependent terms may become important for $T \gtrsim \omega_0$. Corrections of the order T/J are neglected in our derivation (see [33]) since T/J is small in the relevant temperature range. Another possible source of the T dependence is the multiphonon scattering. Superficially, the two-phonon scattering processes have to be negligible because of the smallness of the spin-phonon coupling discussed above. However, there are factors that can compensate for this smallness. First, the two-phonon scattering is less restrictive, as the transverse phonons can also contribute. Second, in the non-Bravais lattices, the two-phonon processes are also amplified by the number of atoms in a unit cell, N_a. That is, for the single-phonon processes, the number of longitudinal phonons that couple to spins via Eq. (3) is N_a, of which we have chosen only two for our fits in Fig. 3. On the other hand, when a spin-boson scattering is due to the emission or absorption of two phonons, the number of possible processes can be as large as $O(N_a^2)$. A naive and certainly overly optimistic estimate of their number assuming independent polarization and a branch index for each phonon involved in the scattering yields $(3N_a)^2$. In cuprates [42], the total number of phonon modes is large, so this combinatorial factor can be substantial.

A somewhat tedious, but straightforward algebra [33] yields the following result for the two-phonon scattering:

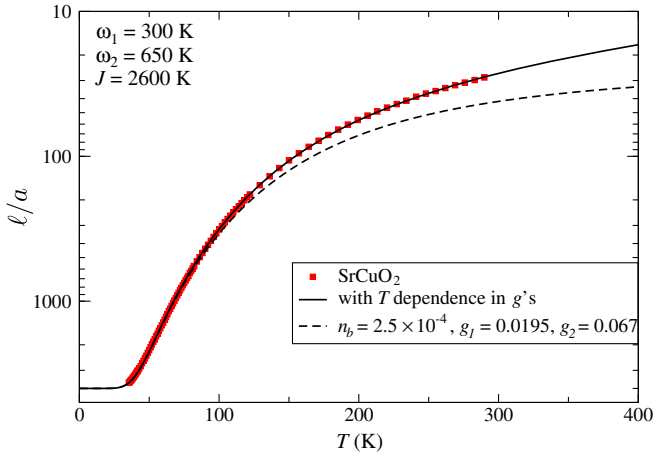

FIG. 4. Same as in Fig. 3. The solid line includes T dependence in the spin-phonon coupling; see the text.

$$\left(\frac{\ell_{\rm sp,2}}{a}\right)^{-1} = g_{\rm sp,2}^2 \frac{J}{T}\frac{\cosh(\omega_0/T)}{\sinh^2(\omega_0/T)}, \tag{11}$$

where $g_{\rm sp,2}^2 \propto C_2 g_{\rm sp}^4$. When compared to Eq. (10), the result in Eq. (11) contains an extra factor, $g_{\rm sp}^2 \sim 0.01$, and a large combinatorial factor, C_2. Clearly, at $T \ll \omega_0$, the two-phonon mean-free path follows the same behavior as Eq. (10), thus simply renormalizing single-phonon scattering. However, at $T \gtrsim \omega_0$, it carries an extra power of T/ω_0, $(\ell_{\rm sp,2}/a)^{-1} \approx g_{\rm sp,2}^2 JT/\omega_0^2$, thus amounting to an expansion in $T/\omega_{0,i}$, which can be argued to follow naturally from the multiphonon scattering processes.

Without going into nongeneric microscopic considerations, one can suggest a simple ansatz to account for the $T/\omega_{0,i}$ expansion with the T dependence of the spin-phonon coupling in the form $g_{\rm sp,i}(T) = g_{\rm sp,i}(1 + r_i n_{0,i})$, where $n_{0,i} = 1/(e^{\omega_{0,i}/T} - 1)$ as before. This form meets both the low-T and the high-T behavior of the two-phonon mean-free path discussed above. A fit of the $SrCuO_2$ data using this ansatz with $r_i = 1$ is provided in Fig. 4. The bare spin-phonon coupling constants $g_{i,\rm sp}$ are even smaller than in Fig. 3, especially for the higher-energy mode. The result with the bare $g_{i,\rm sp}$'s is provided for comparison. Although this figure is an illustration showing that our theory allows for systematic extensions by including multiphonon processes, it also demonstrates a potential role of the latter in the $T \gtrsim \omega_0$ regime and thus contributes to the general description of the heat transport in spin-chain materials.

Conclusions.—We have provided a consistent microscopic theory for thermal transport and scattering in 1D spin chains which stands out from previous attempts at such a theory by having weak spin-phonon coupling and conforming to the analogy of the phonon scattering to that on impurities. We have successfully fit the available experimental data and discussed possible extensions of our theory for higher T. Our approach should be applicable to the thermal conductivity in spin-ladder materials and can

be extended to the transport phenomena in a variety of Luttinger liquids and ultracold atomic gases. Numerical verification of our results is also called for.

We would like to thank Christian Hess for sharing his previously published data and for the numerous fruitful and enlightening discussions. A. L. C. also thanks Andrey Zheludev for his patience, unabating constructive criticism, and useful suggestions. Work of A. L. C. was supported by the U.S. Department of Energy, Office of Science, Basic Energy Sciences under Award No. DE-FG02-04ER46174. A. L. C. would like to thank KITP UC Santa Barbara, where part of this work was done, for their hospitality. The work at KITP was supported in part by the National Science Foundation under Grant No. NSF PHY11-25915. A. V. R. acknowledges the support of RFBR through Grants No. 14-02-00276-a and No. 15-02-02128, and of the Russian Science Support Foundation.

[1] P. Jordan and E. Wigner, Z. Phys. **47**, 631 (1928).
[2] H. Bethe, Z. Phys. **71**, 205 (1931).
[3] R. Nandkishore and D. A. Huse, Annu. Rev. Condens. Matter Phys. **6**, 15 (2015); A. Pal and D. A. Huse, Phys. Rev. B **82**, 174411 (2010).
[4] A. O. Gogolin, A. A. Nersesyan, and A. M. Tsvelik, *Bosonization and Strongly Correlated Systems* (Cambridge University Press, Cambridge, England, 1998).
[5] S. R. White, Phys. Rev. Lett. **69**, 2863 (1992); U. Schollwöck, Rev. Mod. Phys. **77**, 259 (2005).
[6] B. Lake, D. A. Tennant, C. D. Frost, and S. E. Nagler, Nat. Mater. **4**, 329 (2005); I. A. Zaliznyak, Nat. Mater. **4**, 273 (2005); D. A. Tennant, T. G. Perring, R. A. Cowley, and S. E. Nagler, Phys. Rev. Lett. **70**, 4003 (1993); S. E. Nagler, D. A. Tennant, R. A. Cowley, T. G. Perring, and S. K. Satija, Phys. Rev. B **44**, 12361 (1991).
[7] A. Zheludev, M. Kenzelmann, S. Raymond, E. Ressouche, T. Masuda, K. Kakurai, S. Maslov, I. Tsukada, K. Uchinokura, and A. Wildes, Phys. Rev. Lett. **85**, 4799 (2000).
[8] I. A. Zaliznyak, H. Woo, T. G. Perring, C. L. Broholm, C. D. Frost, and H. Takagi, Phys. Rev. Lett. **93**, 087202 (2004); G. Simutis, S. Gvasaliya, M. Månsson, A. L. Chernyshev, A. Mohan, S. Singh, C. Hess, A. T. Savici, A. I. Kolesnikov, A. Piovano, T. Perring, I. Zaliznyak, B. Büchner, and A. Zheludev, Phys. Rev. Lett. **111**, 067204 (2013).
[9] M. B. Stone, D. H. Reich, C. Broholm, K. Lefmann, C. Rischel, C. P. Landee, and M. M. Turnbull, Phys. Rev. Lett. **91**, 037205 (2003).
[10] M. Mourigal, M. Enderle, A. Klöpperpieper, J.-S. Caux, A. Stunault, and H. M. Rønnow, Nat. Phys. **9**, 435 (2013).
[11] T. Giamarchi, *Quantum Physics in One Dimension* (Clarendon Press, Oxford, 2004).
[12] J.-S. Caux and R. Hagemans, J. Stat. Mech. (2006) P12013; J.-S. Caux and J. M. Maillet, Phys. Rev. Lett. **95**, 077201 (2005).
[13] S. R. White and A. E. Feiguin, Phys. Rev. Lett. **93**, 076401 (2004).
[14] S. Langer, F. Heidrich-Meisner, J. Gemmer, I. P. McCulloch, and U. Schollwöck, Phys. Rev. B **79**, 214409 (2009).
[15] S. Langer, M. Heyl, I. P. McCulloch, and F. Heidrich-Meisner, Phys. Rev. B **84**, 205115 (2011).
[16] J. Sirker, R. G. Pereira, and I. Affleck, Phys. Rev. Lett. **103**, 216602 (2009).
[17] J. Sirker, R. G. Pereira, and I. Affleck, Phys. Rev. B **83**, 035115 (2011).
[18] F. Heidrich-Meisner, A. Honecker, D. C. Cabra, and W. Brenig, Phys. Rev. B **66**, 140406 (2002).
[19] S. Grossjohann and W. Brenig, Phys. Rev. B **81**, 012404 (2010).
[20] C. Karrasch, D. M. Kennes, and F. Heidrich-Meisner, Phys. Rev. B **91**, 115130 (2015), and references therein.
[21] X. Zotos, F. Naef, and P. Prelovšek, Phys. Rev. B **55**, 11029 (1997).
[22] F. Heidrich-Meisner, A. Honecker, and W. Brenig, Eur. Phys. J. Spec. Top. **151**, 135 (2007).
[23] X. Zotos, J. Phys. Soc. Jpn. Suppl. **74**, 173 (2005).
[24] E. Shimshoni, N. Andrei, and A. Rosch, Phys. Rev. B **68**, 104401 (2003); **72**, 059903 (2005).
[25] K. Louis, P. Prelovšek, and X. Zotos, Phys. Rev. B **74**, 235118 (2006).
[26] A. L. Chernyshev and A. V. Rozhkov, Phys. Rev. B **72**, 104423 (2005); A. V. Rozhkov and A. L. Chernyshev, Phys. Rev. Lett. **94**, 087201 (2005).
[27] N. Hlubek, P. Ribeiro, R. Saint-Martin, A. Revcolevschi, G. Roth, G. Behr, B. Büchner, and C. Hess, Phys. Rev. B **81**, 020405 (2010).
[28] N. Hlubek, P. Ribeiro, R. Saint-Martin, S. Nishimoto, A. Revcolevschi, S.-L. Drechsler, G. Behr, J. Trinckauf, J. E. Hamann-Borrero, J. Geck, B. Büchner, and C. Hess, Phys. Rev. B **84**, 214419 (2011).
[29] N. Hlubek, X. Zotos, S. Singh, R. Saint-Martin, A. Revcolevschi, B. Büchner, and C. Hess, J. Stat. Mech. (2012) P03006.
[30] A. Mohan, N. S. Beesetty, N. Hlubek, R. Saint-Martin, A. Revcolevschi, B. Büchner, and C. Hess, Phys. Rev. B **89**, 104302 (2014).
[31] S. Bramwell, J. Phys. Condens. Matter **2**, 7527 (1990).
[32] A. L. Chernyshev and W. Brenig, Phys. Rev. B **92**, 054409 (2015).
[33] See Supplemental Material at http://link.aps.org/supplemental/10.1103/PhysRevLett.116.017204, which includes Ref. [34], for details on the derivation of the spin-phonon scattering rate.
[34] I. S. Gradshteyn and I. M. Ryzhik, *Table of Integrals, Series, and Products*, 5th ed., edited by A. Jeffrey (Academic Press, San Diego, 1994).
[35] P. Jung, R. W. Helmes, and A. Rosch, Phys. Rev. Lett. **96**, 067202 (2006).
[36] J. M. Ziman, *Principles of the Theory of Solids* (Cambridge University Press, Cambridge, England, 1972).
[37] M.-R. Li and E. Orignac, Europhys. Lett. **60**, 432 (2002).
[38] M. Oshikawa and I. Affleck, Phys. Rev. B **65**, 134410 (2002).
[39] C. L. Kane and M. P. A. Fisher, Phys. Rev. B **46**, 15233 (1992).

[40] Within our theory, the T dependence of the mean-free path for the XY version of the model in Eq. (1) does not contain the $1/T$ prefactor in ℓ_{sp}, the feature that can be potentially tested experimentally or numerically.

[41] A. Klümper and D. C. Johnston, Phys. Rev. Lett. **84**, 4701 (2000).

[42] L. Pintschovius, N. Pyka, W. Reichardt, A. Yu. Rumiantsev, N. L. Mitrofanov, A. S. Ivanov, G. Collin, and P. Bourges, Physica (Amsterdam) **174B**, 323 (1991).

[43] P. S. Häfliger, S. Gerber, R. Pramod, V. I. Schnells, B. dalla Piazza, R. Chati, V. Pomjakushin, K. Conder, E. Pomjakushina, L. Le Dreau, N. B. Christensen, O. F. Syljuåsen, B. Normand, and H. M. Rønnow, Phys. Rev. B **89**, 085113 (2014).

[44] A. V. Sologubenko, E. Felder, K. Giannó, H. R. Ott, A. Vietkine, and A. Revcolevschi, Phys. Rev. B **62**, R6108 (2000).

[45] M. Takigawa, O. A. Starykh, A. W. Sandvik, and R. R. P. Singh, Phys. Rev. B **56**, 13681 (1997).